Transport Properties of $La_{0.7}Sr_{0.3}MnO_3/MgB_2$ Random Nanocomposites

Vladimir Tarenkov, Vladimir Krivoruchko, Olha Boliasova

Department of High Pressure Physics and Advanced Technologies
A.A. Galkin Donetsk Institute for Physics and Engineering,
the NAS of Ukraine, Kyiv, Ukraine

Abstract—**We have investigated electrical transport properties of random binary networks composed of superconducting MgB_2 micro-particles and half-metallic ferromagnet $La_{0.7}Sr_{0.3}MnO_3$ nano-particles. Unusually large value of the threshold for a percolation transition to a superconducting state of the nanocomposite has been detected for MgB_2. We explain the observed behavior by significant geometric disparity between particles of the constituents and unconventional (triplet) superconducting state induced in the nanocomposite due to the proximity effect. The effect of high-frequency irradiation on a superconducting transition of the nanocomposite was investigated as well. The influence of a high-frequency signal on the critical current magnitude and superconducting transition of a nanocomposite is revealed. A nonthermal effect of an external electromagnetic irradiation on the nanocomposite characteristics has been found.**

Index Terms—**nanocomposite, percolation transition, proximity effect, Josephson junctions**

I. Introduction

The first realization of a Josephson junction utility as tunable microwave sources and detectors can be traced back to the earliest works by Josephson. It was also very early realized that a single Josephson junction emits too little energy to be useful as a microwave source. This and other shortcomings can be eliminated by employing arrays of Josephson junctions. Such arrays can be obtained by creating structures representing a composition of a superconductor (S) separated by normal inclusions. In this case, it is possible to obtain a set of superconductor-normal metal-superconductor (S-N-S) contacts. Sensitivity of current-voltage (I-V) characteristics of the S-N-S contacts to high-frequency electromagnetic fields is due to a superconducting proximity effect. Namely, the proximity induced phase-coherent state is established between superconducting sides of the contact and thus the Cooper pairs flow through the normal interlayer. When a magnetic or electromagnetic field is applied to a contact, the phase coherence between the contact's sides is broken and a contact transfers into a resistive state. In this case, the I-V characteristic of a contact demonstrates the absence of a critical current and a strong nonlinearity at low voltages, $V < V_c = I_cR_n$, on the contact (here I_c is the critical current of the contact, R_n is the contact resistance in a normal state). With increasing of an electromagnetic radiation, the nonlinearity of I-V characteristics of the contact in the V_c region is rapidly suppressed and the contact transfers into a normal state. In practice, when conventional Ss are used, V_c does not exceed several dozen microvolts. This circumstance strongly limits the dynamic range of Josephson junction functionality and thus its applicability in devices. To expand the dynamic range and significantly enlarge magnitude of V_c, it is proposed to use a three-dimensional structure of weekly coupled contacts - the so-called 3D Josephson medium. The creation of such a medium can be realized artificially by means of a direct contact of various materials with superconducting material. As a result, new compounds with unique characteristics not realized for 'parent' components can be obtained [1-7]. In particular, interest to superconducting proximity effect in S-N structures is initiated by the possibilities of new applications of these structures as novel functional elements of nanoelectronics [1-3].

One of such S-N 3D Josephson medium nontrivial implementation can be a composite of a half-metallic ferromagnet (hmF) with an S metal. Indeed, an existence of proximity effect in hybrid hmF and high-T_C S film's structures has been demonstrated in Refs. [8-11]. Long-range proximity effect and induced superconducting order in such hmF as manganites was detected, in particular, by Andreev reflection in experiments on the manganite-S point contacts [12-15] (manganite = $La_{0.7}Ca_{0.3}MnO_3$, $La_{0.7}Sr_{0.3}MnO_3$, S = Pb, Nb, MgB_2). In addition to the spectroscopic manifestation of the proximity effect in contacts of an S with manganites, a superconducting current has been detected in numerous studies of hybrid S-manganite-S film's structures [8-11,16]. Overall, the superconducting proximity effect was observed in half-metallic manganites being in contact with Ss of different symmetries: as *s*-wave symmetry Pb, Nb, MgB_2 [12-14], as well as *d*-wave symmetry, cuprates [8-11,16,17], of the order parameter. Yet, the question, what mechanism is responsible for the transfer of Cooper pairs through the hmF remains still open and is the subject of intensive discussions [1,3,4,5].

II. Experiment

We have studied transport properties of superconductor (MgB_2) – hmF (manganite $La_{0.7}Sr_{0.3}MnO_3$, LSMO) composites with different bulk contents of the components. The specific feature of the composites was that MgB_2 is a powder of a micrometer size (5-10 μm), while LSMO is a nanometer powder with an average particle size about 20-30 nm. The homogeneous composition of the samples was obtained by

The work was supported by the grant of the State Fund for Fundamental Research of the Ukraine (project No: F76/35-2018).

mixing the components in alcohol, followed by drying and additional mechanical mixing. From the resulting mixture, plates with the dimension S = 0.2*1*10 mm^3 were prepared at pressures of 40-60 kbar. The current and potential measuring contacts were prepared by pressing the plates with fine-dispersed silver in the contact's area. Resistance of the contact pads was R = 10^{-3} Ω and was practically independent on the composite composition. As a proof of a homogeneous distribution of the components over a volume of the sample we attract attention to the fact that the resistance of various plates of the same composition is equal, and a linear dependence of the resistance on the length of the plate region, which was obtained with the help of six potential contacts. The samples were not additionally sintered to avoid mutual diffusion and chemical reactions of the components. Thus, the nanocomposites under consideration are random mixtures of two components.

As is known, the electric transport characteristics of composites depend not only on the properties of its constituent elements, but also on the structure of the percolation cluster that appears in the composite [18]. Special case is when the components greatly differ on their conductivity [3]. If an infinite (percolate) conducting cluster over a highly conductive component of the composite is broken, the transport characteristics of the composite will be determined by a high-resistive phase.

In the LSMO/MgB_2 composite, the high-resistive phase is LSMO and the low-resistive phase is MgB_2. By varying the concentration (p) of LSMO, it enables to define a threshold (p_c) above which the transport characteristics of the composite are determined by the current flow through chains – LSMO – MgB_2 – LSMO – MgB_2 –. For the samples with $p > p_c$ the observation of a superconducting current is the evidentiary fact of the superconducting proximity effect in manganite LSMO.

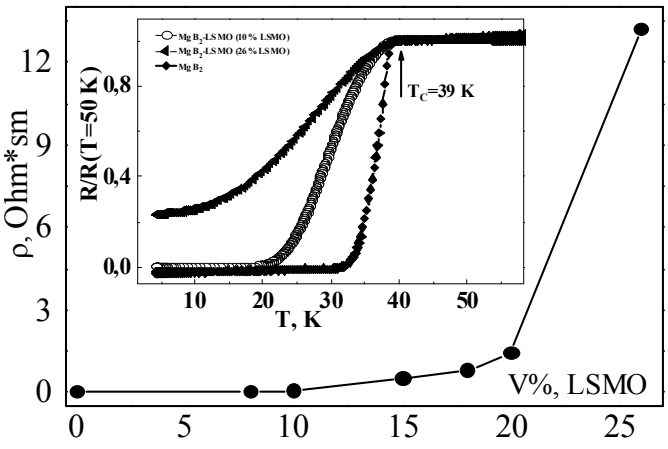

Figure 1. Dependence of the resistivity of the nanocomposite on the volume content of LSMO; T = 300 K. Inset: temperature dependences of the resistances normalized to R(T = 50 K), MgB_2, nanocomposite (10% and 26% of LSMO).

III. Experimental Results

Fig. 1 shows the dependence of the LSMO/MgB_2 nanocomposite resistivity on the volume content of LSMO at temperature T = 300 K. A rapid change in the sample's resistivity occurs in the region of 20% volume concentration of LSMO. The temperature dependence of the resistance for pure MgB_2 and a composite with 10% and 26% LSMO volume content is shown in the inset in Fig. 1. It can be seen from the figure that already 10% of LSMO substantially broadens the resistive superconducting R(T) transition of the composite as compared to the pure MgB_2 sample. The resistance of the sample with 26% LSMO in MgB_2 remains finite throughout the temperature range under study, although the onset of the R(T) decrease coincides with the T_C of pure MgB_2. Note that the resistance-versus-temperature dependences were taken from transport current values that do not affect the R(T) transition behavior.

Based on the traditional models [18] of a percolation transition in the sense of geometric contact, small additions of LSMO can not affect the formation of a MgB_2 infinite cluster since in the case of equal-size components its formation is achieved already at 20% of magnesium diboride. However, in our case, the percolation path per MgB_2 is disturbed due to a significant difference in the particle sizes of MgB_2 and LSMO (5-10 μm and 20-30 nm, respectively). Indeed, due to the mixing and pressuring, the manganite nanoparticles envelop the MgB_2 microcrystals. As a result, a direct contact of the MgB_2 granules is eliminated and the resistance of the composite is determined by the – LSMO – MgB_2 – LSMO – MgB_2 – chains, which leads to a significant broadening of the R(T) curve.

The results of the sample density measurements after pressing support this assumption. The density of MgB_2 plates obtained at pressures of 40 - 60 kbar was (72 ± 3)% of the single crystal MgB_2. The density of the compacted LSMO nano-powder at the same pressures was only (68 ± 3)% of the LSMO; the density of the MgB_2 - LSMO composite (26% of LSMO) was (96 ± 3)% of the calculated density. Such high density of the composite points that the LSMO nano-powder under high uniaxial pressures "spreads" throughout the sample volume, filling the pores around large MgB_2 granules.

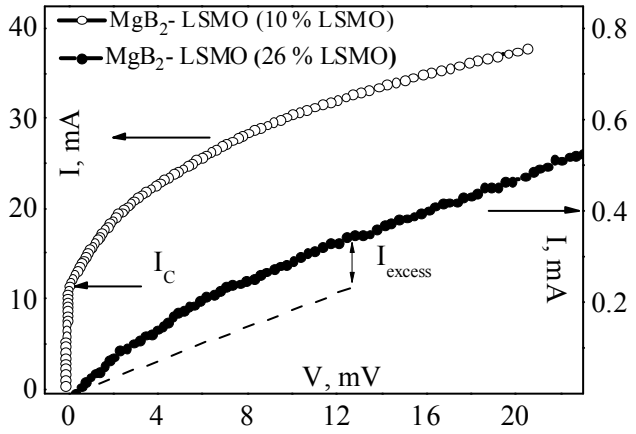

Figure 2. Current-voltage characteristics of LSMO/MgB_2 nanocomposites with 10% and with 26% LSMO content.

Fig. 2 shows the I-V characteristics of the LSMO/MgB_2 samples (10% and 26% of LSMO). The critical current, I_C, is

observed at 10% of LSMO, but for 26% of LSMO the I-V dependence does not exhibit the presence of a critical current. Yet, it has a shape typical for a medium of weakly coupled contacts with an excess current, i.e., the current in the superconducting state exceeds the current in the normal state. These results most naturally can be interpreted in terms of a 3D Josephson medium - a bulk of a large number of Josephson S-N-S contacts.

An effective way to show the nature of the current flow in the composite is the response of its transport characteristics on a hydrostatic pressure. It is well known that for any structure of a grid of weakly connected S-N-S contacts their superconducting characteristics will be improved under the pressure effect. It follows from the exponential dependence of a current through a weak connection from its thickness d, $I \approx I_C \exp(-d/\xi_n)$, ξ_n is the coherence length of the N layer.

We carried out experiments on high hydrostatic pressures effect on the temperature dependence of the superconducting transition and the critical current of the nanocomposites. Samples of LSMO/MgB_2 nanocomposites with a volume concentration of 26% LSMO were placed in a high-pressure chamber of a piston-cylinder type. The pressure transfer medium was a kerosene-oil mixture. In addition to the composite sample, a platinum wire temperature sensor and a pressure sensor were placed in the chamber.

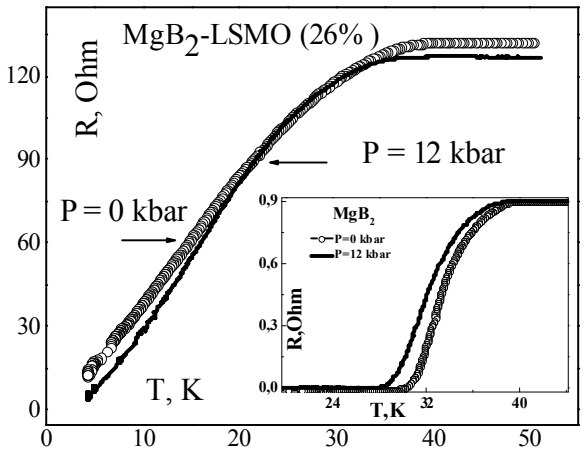

Figure 3. Effect of hydrostatic pressure on the temperature dependence of the resistivity of a nanocomposite (26% LSMO). Inset: the effect of pressure on the temperature dependence of the MgB_2 resistance.

In Fig. 3, the resistivity-versus-temperature dependences are shown for the sample LSMO/MgB_2 (26% LSMO) at zero (atmosphere) and P = 12 kbar pressures. Under the influence of pressure, the beginning of the transition shifted toward low temperatures, and the smearing region, starting from the middle of the R(T) transition, shifted to high temperatures. Such pressure effect on the temperature dependence of the composite resistance is determined by two factors – a negative value of dT_C/dP for MgB_2 and a response of the intergranular regions to the pressure. The inset in Fig. 3 shows the influence of pressure on the dependence of the superconducting R(T) transition for pure MgB_2. Under the effect of pressure, the critical transition temperature drops with a rate of $dT_C(P)/dP \approx 0.1$ K/kbar. Note that the dT_C/dP value for MgB_2 obtained for our compacted samples is in the complete agreement with the data given in Ref. [19] for pure magnesium diboride. The decreased smearing of the R(T) curve for the composite appears due to the decrease in the resistance of the LSMO grains in the MgB_2-LSMO-MgB_2 contacts, which is reflected in the decrease of the composite total resistance under pressure. The same result was also displayed in the I-V characteristics of MgB_2 and nanocomposite samples. In Fig. 4, dependence of the nanocomposite I-V characteristics on the applied pressure are shown. Under pressure, the critical current of the composite increased, i.e., the resistance of the sample decreased. The inset in Fig. 4 shows the dependence of the I-V characteristic for pure MgB_2. It can be seen that in this case the behavior is opposite: the critical current decreases under pressure. Thus, the experiments on the pressure effect on the LSMO/MgB_2 nanocomposite transport characteristics prove the formation of a structure of weakly coupled S-N-S type contacts in the composite.

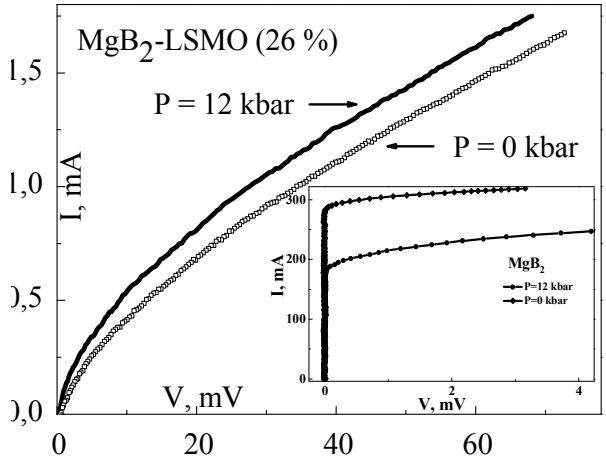

Figure 4. The effect of a hydrostatic pressures on the current-voltage characteristic of a nanocomposite (26% LSMO). Inset: the effect of pressure on the current-voltage characteristic of MgB_2.

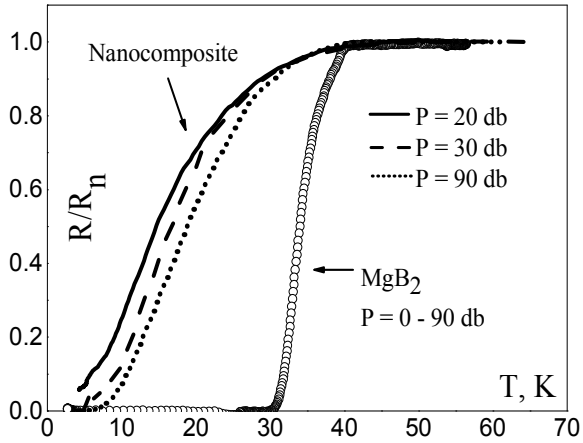

Figure 5. Effect of a high-frequency irradiation on the resistive superconducting transition of the LSMO/MgB_2 composite (26 % LSMO).

As is known, in the ferromagnetic phase, manganites are the so-called half-metals, in which carriers with only one direction of spins present at the Fermi level. For such

compounds, one cannot expect the realization of the classical *s*-wave proximity effect because there is no possibility to form a Cooper pair with zero total spin. However, if the surface layer of a manganite is spin-active, it provides possibility to transform Cooper pairs with the s-wave symmetry of the order parameter into Cooper pairs with the *p*-wave symmetry [1,20-22]. Then through the S-hmF-S contacts a spin-polarized current of *p*-wave Cooper pairs can flow. It is of interest to study dynamic characteristics of such contacts. In particular, as is known, in conventional S-N-S contacts the formation of so-called Josephson vortices - closed superconducting ring currents – takes place [23]. Unlike Abrikosov vortices, Josephson vortices do not have a normal core. Therefore, the frequency range of the electromagnetic signal that causes a response in typical characteristics of the Josephson medium is very wide and is limited only by the superconducting energy gap.

We have investigated the effect of a high-frequency irradiation, f = 50 MHz, on the composite I-V characteristics. The irradiation was supplied from the main output of the generator G4-102 with a voltage V_{max} = 0.5 V. The signal has been fed to the sample through a capacitance C = 0.1μF along a thin measuring wire.

Fig. 5 illustrates the effect of a high-frequency signal of different amplitudes on the resistive superconducting transition of the LSMO/MgB_2 nanocomposite (27% LSMO). As the amplitude of the applied signal increases, the superconducting transition curve becomes smeared, but the beginning of the transition does not shift. For the pure MgB_2 sample the effect of the high-frequency signal on the critical current value and the superconducting transition has not been detected. It indicates a nonthermal nature of the electromagnetic signal effect on the R(T) characteristic of the nanocomposites under study.

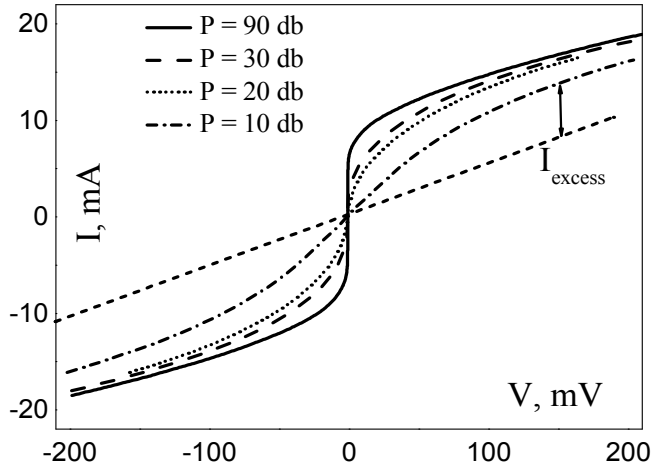

Figure 6. Effect of the radio-frequency irradiation on current-voltage characteristics of the composite (27% LSMO).

The irradiation effect on the I-V characteristic of a nanocomposite sample is shown in Fig. 6. With increasing of external electromagnetic irradiation, the critical current of the sample decreases and the I-V dependence demonstrates a resistive state of the sample but with an excess current.

IV. Conclusion

In conclusion, electrical transport properties of random binary networks composed of micro-particles of the superconductor MgB_2 and nano-particles of half-metallic ferromagnet $La_{0.7}Sr_{0.3}MnO_3$ have been studied. The experimental results show that in the LSMO/MgB_2 nanocomposites the flow of a superfluid current through the half-metallic ferromagnet $La_{0.7}Sr_{0.3}MnO_3$ is realized. It proves that the interface between LSMO and MgB_2 is a spin-active region, i.e., passing through this region Cooper pair with *s*-wave symmetry of the order parameter can be transformed into a pair of *p*-wave (triplet) symmetry and flows through the ferromagnetic half-metal. We argue that the constituent particle geometrical size and indirect interaction via proximity effect play a crucial role to achieve the necessary conditions enabling a superconducting percolation transition in the nanocomposites under consideration. The unusual transport properties of this type of nanocomposites bear much fundamental interest and are of potential interest for future applications, e.g. as novel functional materials for microwave radiation detection.

References

[1] M. Eschrig, Phys. Today vol. 64, p. 43, 2011.
[2] X.-L.Qi, S.-C. Zhang, Rev. Mod. Phys., vol. 83, p. 1057, 2011.
[3] X. Liu, R. P. Panguluri, Z.-F. Huang, B. Nadgorny, Phys. Rev. Lett., vol. 104, 035701, 2010.
[4] F. S. Bergeret, A. F. Volkov, K. B. Efetov, Rev. Mod. Phys., vol. **77**, p. 1321, 2005.
[5] A. I. Buzdin, Rev. Mod. Phys., vol. 77, p. 935, 2005.
[6] I. F. Lyuksyutov, V. L. Pokrovsky, Adv. Phys., vol. 54, p. 67, 2005.
[7] A. Bawa, A. Gupta, S. Singh, V.P.S. Awana, S.Sahoo, Sci. Rep., vol. 6, 18689, 2016.
[8] Z .L. Zhang, U. Kaiser, S. Soltan, H-U. Habermeier, B. Keimer, Appl. Phys. Lett., vol. 95, 242505, 2009.
[9] G. Koren, T. Kirzhner, Phys. Rev. B, vol. 84, 134517, 2011.
[10] D.K. Satapathy, M.A. Uribe-Laverde, I. Marozau, V.K. Malik, S. Das, Th. Wagner, et al., Phys. Rev. Lett., vol. 108, 197201, 2012.
[11] Y. Kalcheim, T. Kirzhner, G. Koren, O. Millo, Phys. Rev. B, vol. 83, 064510, 2011.
[12] V. Krivoruchko, V. Tarenkov, Phys. Rev. B, vol. 75, 214508, 2007.
[13] V. Krivoruchko, V. Tarenkov, Phys. Rev. B, vol. 78, 054522, 2008.
[14] V. Krivoruchko, V. Tarenkov, Phys. Rev. B, vol. 86, 104502, 2012.
[15] V. Krivoruchko, A. D'yachenko, V. Tarenkov, Low Temp. Phys., vol. 39, p. 276, 2013.
[16] G. Koren, T. Kirzhner, Phys. Rev. B, vol. 84, 134517, 2011.
[17] M. Kasai, Y. Kanke, T. Ohno, Y. Kozono, J. Appl. Phys., vol. 72, p. 5344, 1992.
[18] A. Bunde, W. Dieterich, J. Electroceram, vol. 5, p. 81, 2000.
[19] C. Buzea, T. Yamashita, Supercond. Sci. Technol, vol. 14, R115, 2001.
[20] J. Linder, A. Sudbø, T. Yokoyama, R. Grein, M. Eschrig, Phys. Rev. B, vol. 81, 214504, 2010.
[21] Y. Tanaka, M. Sato, N. Nagaosa, J. Phys. Soc. Jpn., vol. 81, 011013, 2012.
[22] F. Hübler, M. J. Wolf, T. Scherer, D. Wang, D. Beckmann, H. V. Löhneysen, Phys. Rev. Lett., vol. 109, 087004, 2012.
[23] M. Tinkham, "Introduction to Superconductivity", McGraw-Hill, New York, 1996, 2nd ed.